

Gamma-ray Spectrometry of Soil Samples from the Provincia dell'Aquila (Central Italy)

E. Bellotti^{a,b}, G. Di Carlo^{b,c}, D. Di Sabatino^d, N. Ferrari^c, M. Laubenstein^c
L. Pandola^c, C. Tomei^c

Submitted to Applied Radiation and Isotopes

INFN - Laboratori Nazionali del Gran Sasso

*Published by SIS-Pubblicazioni
dei Laboratori Nazionali di Frascati*

Gamma-ray Spectrometry of Soil Samples from the Provincia dell'Aquila (Central Italy)

E. Bellotti^{a,b}, G. Di Carlo^{b,c}, D. Di Sabatino^d, N. Ferrari^c, M. Laubenstein^c
L. Pandola^c, C. Tomei^c

^a *Università di Milano Bicocca and INFN,
Piazzale delle Scienze 3, I-20126 Milano, Italy*

^b *Consorzio di Ricerca Gran Sasso,
S.S. 17 bis km 18+910, I-67010 Assergi (AQ), Italy*

^c *Laboratori Nazionali del Gran Sasso INFN,
S.S. 17 bis km 18+910, I-67010 Assergi (AQ), Italy*

^d *c/o Università dell'Aquila, Dipartimento di Scienze Ambientali,
Via Vetoio 1, I-67010 Coppito (AQ), Italy*

Abstract

In the Abruzzo Region (Central Italy) there is a lack of measurements of gamma-ray activity in soils and waters. For this reason, we have planned to carry out a systematic measurement of soils in the area of the Provincia dell'Aquila, which covers about one half of the entire region. In this paper we report the results obtained from 56 soil samples, collected in the northern part of the area of interest (about one fourth of the total area under study). The results, in terms of content of uranium, thorium and potassium and the activity of caesium are reported, as well as the details on the experimental procedure. The results show a limited content of K and U, with no large variations from site to site, in agreement with the expectations based on the knowledge of the geo-lithological nature of the soil. The amount of Th is also quite limited, with a few exceptions where the Th content is up to five times the average value. Caesium, originated from the fall-out following the Chernobyl accident, is very irregularly distributed owing to the complicated orography of the land. Future plans are also shortly discussed.

1 Introduction

In many countries scientific institutions, public and private organisations have stimulated the collection of a large variety of data and their classification in thematic maps which give a useful and synthetic description of the land. Radiometric data, usually obtained by γ -ray spectrometry, have been collected in many areas around the world. The aims of these measurements cover many different scientific and practical interests, ranging from basic geophysics to mineral exploration and environmental radiation monitoring.

Data have been collected mainly using two techniques: measurements of γ -ray activity in soil and water samples and airborne γ -ray measurements. It is outside the scope of the present paper to give a complete list of all the available data. Let us cite only a few of them: the Canadian Natural Resources Organisation promoted a wide program of measurements, also in the field of natural radioactivity, over a large fraction of Canada (information can be found in http://gsc.nrtcan.gc.ca/gamma/appgeo_e, where also a rich reference list is reported); in Italy a few areas have been investigated, namely: the Alps-Appennine transition region (Chiozzi et al. 2002), Ustica (Bellia et al. 1997) and the Pantelleria Island in Southern Italy (Brai et al. 1995); data for Switzerland are reported in (Rybach et al. 1996), for Cyprus in (Tzortzis et al. 2003), for India in (Singh et al. 2005).

To our knowledge, there is a lack of similar data for the Abruzzo Region, in Central Italy. Therefore, we initiated a campaign of measurements on the radioactivity content of soils in a limited area - the Provincia dell'Aquila - to evaluate the feasibility of a wider systematic campaign. In this paper we report the results of γ -ray spectrometry on 56 samples of soil regularly distributed over an area of about 1300 km².

The paper is organised as follows: sect. 2 gives a short description of the geological nature of the interested area, sect. 3 describes the sample collection and the measurements in situ, sect. 4 describes the sample laboratory measurements and data analysis, sect. 5 presents the results and their interpretation and sect. 6 the outlook and conclusions.

2 Short description of the geological nature of the interested area

The region considered in this paper is the Provincia dell'Aquila in the Abruzzo Region (Central Italy); note that the denomination of Provincia is of administrative origin, not strictly related to any special geological or orographical structure of the land. The extension of this area is about 5000 km²; it is moderately populated (60 inhabit./km²); mountains, high up to 3000 m a.s.l. cover a large fraction of this area.

This study is focused on a portion of the Abruzzo Apennines chain, located between the Gran Sasso and the Sirente-Velino massifs. From a geological point of view, the Sirente-Velino Unit belongs to the "Latium-Abruzzo Carbonatic Platform" and it is constituted by carbonatic platform and reef edge lithofacies.

The structure is thrust towards North-East on the Mio-Pliocenic deposits and outcrops

like a South-West dipping monocline. The Gran Sasso Unit represents the northernmost section of the Abruzzo Carbonatic arc and presents a Meso-Cenozoic sequence typical of a basin transitional environment. This structural Unit overlaps the silicoclastic deposits referred as fore arc sediments of Laga Fm. (Messinian-Lower Pliocene).

The tectonic and morpho-structural setting of Gran Sasso is characterised mainly by NW-SE and E-W oriented faults, whose extensional activity has determined the formation of tectonic intermontane basins (i.e. the "Conca Subequana") filled with Quaternary fluvial-lacustrine sediments (see Fig. 1).

Structures of this kind show a limited content of U and Th; however anomalous contents of Th/U bearing minerals (monazite, zircon, britholite, cheralite, pyrochlore) have been observed within the Quaternary sediments, giving rise to a gamma activity higher than expected (Di Sabatino 2006). The source of radioactivity must be looked for mainly in the volcanic ashes and pyroclastics coming from the Tuscan-Latinal magmatic Plio-Pleistocenic province. These volcanic sediments occur in horizons interbedded into Quaternary sequences but more often they are re-worked by runoff waters and re-sedimented in morpho-structural traps. For a reference on the geology of the Abruzzo Region see (Accordi et al. 1988, Vezzani et al. 1998).

3 Sample collection and measurements in situ

The radioactive elements of major interest for this kind of measurements are ^{238}U and ^{235}U and their daughters, ^{232}Th and its daughters, ^{40}K and ^{137}Cs . We searched for caesium because this area was interested by the fall-out originated by the Chernobyl accident (UNSCEAR 2000). The presence of the above listed elements in soils and waters can be detected and evaluated quantitatively by γ -ray spectrometry. To this purpose, we have followed the procedure described below.

We have superimposed to the topographical map of the Provincia dell'Aquila a square grid of 5 km side. This was purposely a "blind" grid, in order not to be influenced by any a priori consideration on the nature of the soil. This choice has been considered the less biased possible for a preliminary survey of the content of radioactive elements.

In each point of the grid (198 points in total) we have collected or we plan to collect a sample of soil. In this paper we report the results obtained on 56 samples collected in the northern part of the Provincia (see Fig. 2); they cover about 1/4 of the total area.

In 23 of these points, a gamma ray spectrum was collected in situ by means of a portable NaI detector (Canberra Inspector 1000) especially designed for environmental screening and for field measurement applications requiring dose and count rate measurements. It provides features as nuclide identification and activity measurements as well as spectrum acquisition and analysis.

The samples, about 1 kg each, were collected a few cm below the surface; organic materials and pebbles approximately larger than one cm^3 were eliminated. They have been naturally dried and then inserted in sealed plastic boxes, 500 cm^3 volume. Activity measurements were carried out at least two weeks later.

4 Laboratory measurements and data analysis

4.1 Experimental set up and sample measurements

Samples have been measured by means of a 3"×3" NaI crystal (model 905-4 provided by Ortec). The detector has been installed above ground in the external buildings of the Gran Sasso National Laboratory (LNGS) of INFN, enclosed in a 40×40×60(height) cm³ shielding of fairly radio pure lead. The lead on top of the detector was excavated to allow a precise positioning of samples. Special care has been taken to minimise the volume of air around the sample boxes. A few samples have been also measured with a similar set-up located deep underground in the Gran Sasso National Laboratory (for a description of this facility see (Arpesella 1996)).

The intrinsic background of the set-up has been routinely measured for a total time of 360 hours; the spectrum obtained by summing partial spectra is shown in Fig. 3. The main contributions to the background are due to cosmic rays, radioactivity from the detector and shielding materials and X-rays, originated in the interactions of radiation within the lead shielding. No significant variations from one background measurement to another have been observed, demonstrating the excellent stability of the background. The global gain of the electronic chain is also stable, allowing the addition of different energy spectra, without need of rebinning.

Each sample has been measured for one day (86400 s). A few samples have been measured twice, with a time interval of many days. The counting rate in the energy interval 0.5 - 3.0 MeV is 0.7 cps for background and it ranges from 1.2 to 11.2 cps for samples. The following sources of signal contribute to the energy spectrum:

- ¹³⁷Cs, which contributes with a single line at 661.6 keV and its Compton tail;
- ⁴⁰K, which contributes with a single line at 1460.8 keV and its Compton tail;
- ²³²Th, ²³⁸U and ²³⁵U, which contribute with many lines, coming from different nuclides of their natural decay chains.

No significant contributions from other radionuclides, e.g. ⁶⁰Co, have been observed.

It must be noted that only some of the elements of the total decay chain of U and Th contribute with detectable lines. In the ²³²Th chain, measurable lines are originated from ²²⁸Ac, ²²⁴Ra, ²¹²Pb, ²¹²Bi and ²⁰⁸Tl. Therefore, this measurement provides an equivalent Th content (Th_{eq}), which is equal to the real Th content under the assumption that secular equilibrium is respected. This is, for natural samples, a very likely assumption.

In the case of ²³⁵U our instrumentation does not allow a quantitative evaluation of its activity, owing to the low isotopic abundance of this nuclide (0.7%), the low energy of the lines and the insufficient energy resolution of NaI. For ²³⁸U, the detectable lines are originated from ²²⁶Ra, ²¹⁴Pb and ²¹⁴Bi. We provide an equivalent U content (U_{eq}) from the detection of Bi and Pb lines. As in the case of Th, the U_{eq} is equal to the content of U only if secular equilibrium is respected, which very often is not the case.

To evaluate the absolute efficiency of our detector, needed to extract the relevant information, namely the content of radionuclides in the sample, we have used both samples of known activity and a Monte Carlo simulation program based on the Geant4 code (Agostinelli et al. 2003). This code, widely used in the fields of high-energy, astroparticle and underground physics, allows to generate primary particles (e^\pm , γ -rays, ions, etc.), propagate them inside a given set-up and reconstruct the energy spectrum deposited inside the sensitive volume (the NaI crystal in our case). The geometry and the materials of the experimental set-up (sample, detector, shielding) must be defined, while the accurate description of the physical process involved (radioactive decay, passage of particles through matter, energy deposition) and the properties of materials are provided by the code.

Ten spectra, one for each of the above listed nuclides, have been simulated assuming the nuclide to be uniformly distributed within the volume of the sample. Simulations have been repeated for 6 different values of the sample mean density, ranging from 0.7 to 1.5 g/cm³, to take into account self-absorption in the sample. The statistics of each simulation (i.e. the number of simulated decays for each nuclide) corresponds to $2 \cdot 10^6$ events; for ⁴⁰K, given its low gamma yield, $10 \cdot 10^6$ events has been simulated.

Adding the simulated spectra of the nuclides belonging to the same chain, scaled with the corresponding branching ratios, we have obtained four "reference spectra" for each component (K, Cs, Th and U). These spectra, in the case of sample density equal to 1.2 g/cm³ are shown in Fig. 4. The accuracy of the simulation is discussed in subsect. 4.3 .

4.2 Spectrum Analysis

Each measured spectrum has been fitted with a "theoretical" spectrum reconstructed from the simulation in the following way:

$$R_i = \alpha K_i + \beta Cs_i + \gamma Th_i + \delta U_i + B_i \quad (1)$$

where K_i , Cs_i , Th_i and U_i are the content in the i -th channel of the simulated spectra. B_i is the expected background in the same channel (as deduced from measurements) and the index i runs over the energy spectrum from 0.5 to 3 MeV. α , β , γ and δ are free parameters. The simulated spectra to be used in the above formula are chosen according to the density of the sample.

Comparing the measured and reconstructed spectra and minimising the χ^2 given by:

$$\chi^2 = \frac{\sum_i (R_i - C_i)^2}{C_i} \quad (2)$$

where C_i is the measured number of counts in bin i , the free parameters are determined. From them, it is straightforward to obtain the concentrations of the considered radionuclides. Fig. 5 shows an example of fitted spectrum compared with the measured one.

4.3 Accuracy

The accuracy of our determination of the content of radionuclides depends on: the statistical fluctuations in the measurements, the accuracy of the Monte Carlo simulations and the effect of self absorption in the sample which is related to its density (see below).

The purely statistical error in evaluating the contribution of the different nuclides to the measured spectrum is extremely small because the entire spectrum is used, instead of the full energy peaks only. In a few cases, the same sample has been measured twice, with a time interval of a few weeks, without finding any significant difference between the obtained results.

The absolute detection efficiency has been measured at the ^{40}K line using a KCl sample, whose content in K is known at the 0.7% level. Measurement and simulation differ by less than 1%. Note that this agreement holds not only for the full energy peak, but also for the Compton tail, down to 250 keV.

We have also measured a non calibrated Th source diffused in a matrix of density 1 g/cm^3 . The comparison of the measured and simulated spectra, appropriately normalised, shows deviations of $\sim 2\%$ in the whole energy range from 0.5 to 3.0 MeV, with the exception of the full energy peaks of the ^{228}Ac lines (at 911, 964 and 969 keV) which are underestimated in the simulation by a 4%.

As mentioned above, the efficiency depends on the density of the sample. As an example, increasing the density by 0.2 g/cm^3 , the efficiency at the Cs line decreases by approximately 5%. Since we have used for each sample a simulated spectrum corresponding to a density close, but not exactly equal to the real one (the maximum deviation is 0.1 g/cm^3) we assume a further contribution to the inaccuracy of 3%, to account for this effect. The overall accuracy attributed to the detection efficiency can be of 7% (at 1σ level). This accuracy reflects itself on the concentration evaluation. A completely different problem is the evaluation of the representativeness of the sample. We will shortly discuss this point in the next section.

5 Results and interpretation

In total, 56 samples have been measured and their content of radionuclides has been determined. Table 1 gives an overall view of our results. It contains the relevant parameters of the samples: the identification number, the longitude, latitude and altitude of the collection point and the geo-lithological group of the sample, according to a classification based on visual inspection. For all the points the latitude is 42° N and the longitude is 13° E , therefore only the minutes and seconds are reported in the table.

Columns 7,8 and 9 in Table 1 report the K, Th_{eq} and U_{eq} content of the sample while column 6 reports the activity of ^{137}Cs in Bq/kg. The concentration (or activity) is then converted into dose. We report separately in Table 1 the dose due to the naturally occurring elements:

$$D_{nat}[\text{nGy/h}] = 5.675 \text{ U}_{eq}[\text{ppm}] + 2.494 \text{ Th}_{eq}[\text{ppm}] + 13.078 \text{ K}[\%], \quad (3)$$

the dose due to caesium:

$$D_{Cs}[\text{nGy/h}] = 0.17 A_{Cs}[\text{Bq/kg}], \quad (4)$$

and the dose due to cosmic rays, computed as a function of the altitude h of the site (in km), following the approach of (UNSCEAR 2000):

$$D_{cr}[\text{nGy/h}] = 32.0 (0.21 e^{-1.649 h} + 0.79 e^{0.4528 h}). \quad (5)$$

The conversion factors in equations 3 and 4 are taken from (IAEA 2003). The three values for the dose are then summed to obtain the total dose in nGy/h, reported in column 13 of Table 1.

The following considerations can be drawn:

- the average abundance of potassium is 0.9%, lower than the mean crust value, as expected from the nature of the soil. In some cases the content is quite low and no anomalously high value has been found. Note that the K content of calcareous rocks from the Gran Sasso massif, as measured by our group with a setup similar to the one described in this work, is as low as 0.2%;
- the values of the uranium concentration range from 0.4 to 5.7 ppm, with a mean value of 2 ppm, in agreement with the average crust abundance;
- the mean value of the thorium concentration is 10 ppm, in rough agreement with the average value for the crust. However there are at least three “anomalies” where the measured activity is 4-5 times larger than the mean one. These points are not geographically close one to the other. It must be noted that localised very strong activities have already been detected in the same area (Di Sabatino 2006);
- the presence of ^{137}Cs has been detected in all the samples. However the variability is very large, ranging from a few Bq/kg up to more than 100 Bq/kg. The mean value is 40 Bq/kg. We want to emphasise that most of the locations are not used for agricultural or other human activities and that our samples have been collected at the surface. If we attribute the presence of caesium to the fall-out due the Chernobyl accident (Arpesella et al. 1995), the observed variability is related to the original deposition of the fall-out, expected to be very uneven due to the orography of the region.

The last column in Table 1 gives the dose measured in situ (when available) with the portable spectrometer, which has to be compared to the dose due to radionuclides. As a matter of fact, the portable instrument is essentially insensitive to the total contribution due to cosmic radiation. Fig. 6 shows the comparison between the doses directly measured and those deduced by the content of radionuclides. We expect some difference between the two values because the portable spectrometer averages the activity of an area of approximately 10 m^2 and 30 cm in depth, while the sample represents the situation of a point and essentially the surface value. As it appears from the figure, there is a correlation between the two measurements and no large systematic effects are detectable. Therefore, we conclude that our data are sufficiently representative of global activity of the region.

6 Outlook and conclusions

Our short term plans, dictated by these preliminary results, are:

- to complete the sampling of the soils;
- to investigate the “anomalous” points, where the contents of Th appears to be significantly higher than in the rest of the grid. That will be done both to define the extension of these areas and to evaluate if there is some relevance with respect to the radio-protection rules;
- to address the question of secular equilibrium for the ^{238}U chain.

On a longer term, we plan to design an airborne study of the radioactivity of the region. As a matter of fact, the orography of the region makes quite difficult the collection of soil samples in a large fraction of the region we would like to map.

From the described results, we can conclude that the investigated area shows a content of naturally occurring radioactive elements in agreement with the expectations from the geo-litological structure of the region. However, note the exception of a few anomalous points. The contamination from ^{137}Cs is still present but obviously has no relevance for radioprotection of the population. More detailed and extensive measurements appear to be of interest for basic geophysics and for environment knowledge.

7 Acknowledgements

We express our gratitude to the Fondazione Cassa di Risparmio della Provincia dell’Aquila, who partly funded this work; the support of the technical staff of LNGS is warmly acknowledged; we are grateful to Mrs. S. Fattori for her help in the sample measurements and data analysis; we thank also our colleagues C. Broggin, G. Fiorentini, C. Rossi Alvarez and C. Salvo for many enlightening discussions. We acknowledge the funding from the EU FP6 project ILIAS.

References

- [1] G. Accordi et al., *Note illustrative alla carta delle litofacies del Lazio-Abruzzo ed aree limitrofe*, Prog. Fin. Geodinamica, Quaderni de *La Ricerca Scientifica*, C.N.R., 114 (5): 223 p., Roma (1988).
- [2] S. Agostinelli et al., *GEANT4: A Simulation Toolkit*, Nucl.Instrum. Meth **A506** (2003) 250-303.
- [3] C. Arpesella and G. Schirripa Spagnolo, *Monitoraggio del Radon e della Ionizzazione*, Internal Report Consorzio Ricerca Gran Sasso 1995.

- [4] C. Arpesella, *A low background counting facility at Laboratori Nazionali del Gran Sasso*, Appl. Rad. and Isotop. **47** (1996) 991-996.
- [5] S. Bellia, M. Brai, S. Hauser, P. Puccio, S. Rizzo, *Natural radioactivity in a volcanic island Ustica, Southern Italy*, Appl. Radiat. Isot. **48** (1997) 287-293.
- [6] M. Brai et al., *Natural radiation of rocks and soils on the island of Pantelleria*, Health Phys. **63**, vol. 3 (1995) 356-259.
- [7] P. Chiozzi, V. Pasquale, M. Verdoya, *Naturally occurring radioactivity at the Alps-Appennines transition*, Radiation Measurements **35** (2002) 147-154.
- [8] D. Di Sabatino, *Evoluzione delle forme morfosedimentarie in funzione della qualità ambientale (radioattività naturale)*, Ph. Thesis, Università dell'Aquila (2006).
- [9] IAEA, *Guidelines for radioelement mapping using gamma ray spectrometry data*, IAEA-TECDOC-1363 (2003).
- [10] L. Rybach, G.F. Schwarz and F. Medici, *Construction of radioelement and dose-rate baseline map by combining ground and airborne radiometric data*, Contribution n. **913**, Institute of Geophysics ETH Zurich, 1996.
- [11] S. Singh, A. Rani and R.K. Mahajan, Radiation Measurement **39** (2005) 431-439.
- [12] M. Tzortzis, H. Tsertos, S. Christofides and G. Christodoulides, *Gamma-ray measurements of naturally occurring radioactive samples from Cyprus characteristic geological rocks*, Radiation Measurement **37** (2003) 221-229.
- [13] UNSCEAR, *Sources and effects of ionizing radiation*, Report to the General Assembly, with Scientific Annexes, United Nations, New York (2000).
- [14] L. Vezzani and F. Ghisetti, *Carta geologica dell'Abruzzo*, Regione Abruzzo, Settore Urbanistica-Beni ambientali e Cultura, S.E.L.CA., Firenze (1998).

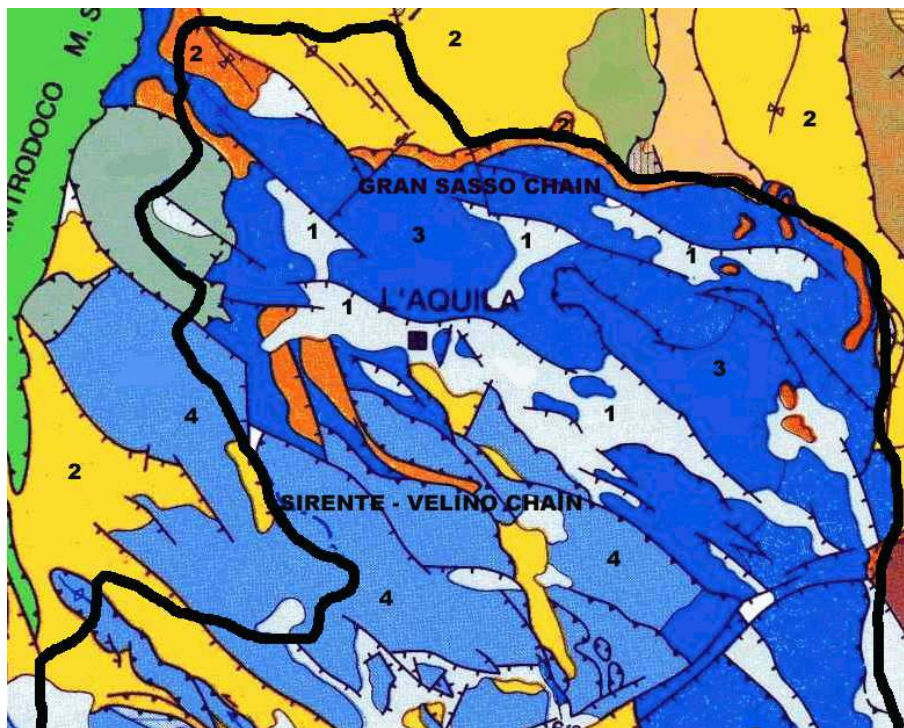


Figure 1: Geo-lithological map of the northern part of the Provincia dell'Aquila. Legend: 1) Marine and continental Plio-Quaternary deposits; 2) Upper Miocene siliciclastic flysch deposits; 3) Meso-Cenozoic carbonate sedimentary Units.

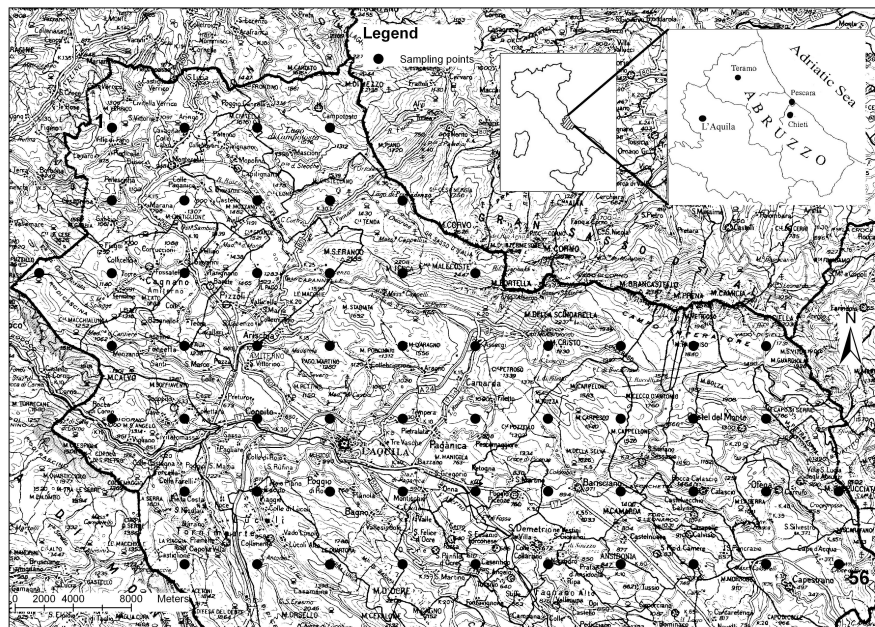


Figure 2: Topographical map of the Provincia dell'Aquila with the indication of the sampling points.

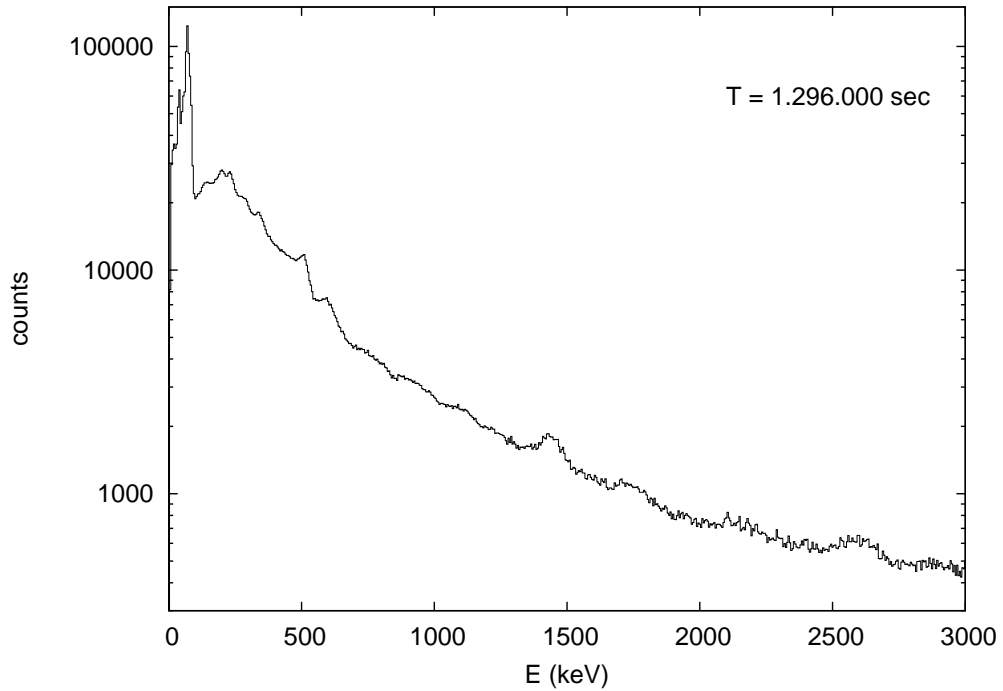


Figure 3: Background spectrum of the NaI detector, corresponding to a measuring time of 15 days.

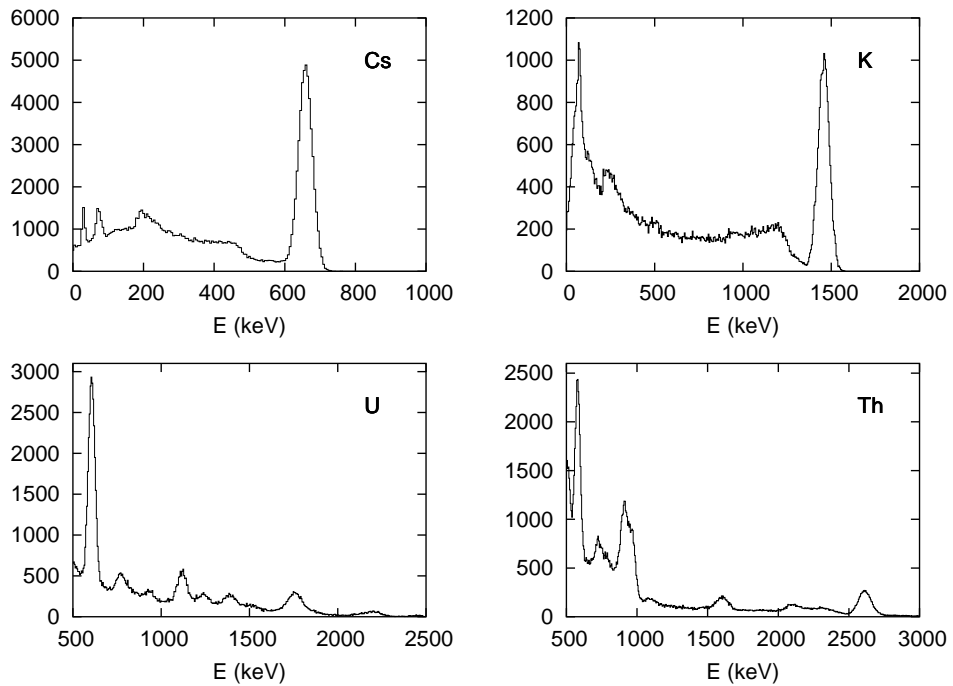


Figure 4: Simulated spectra of the four radioisotopes.

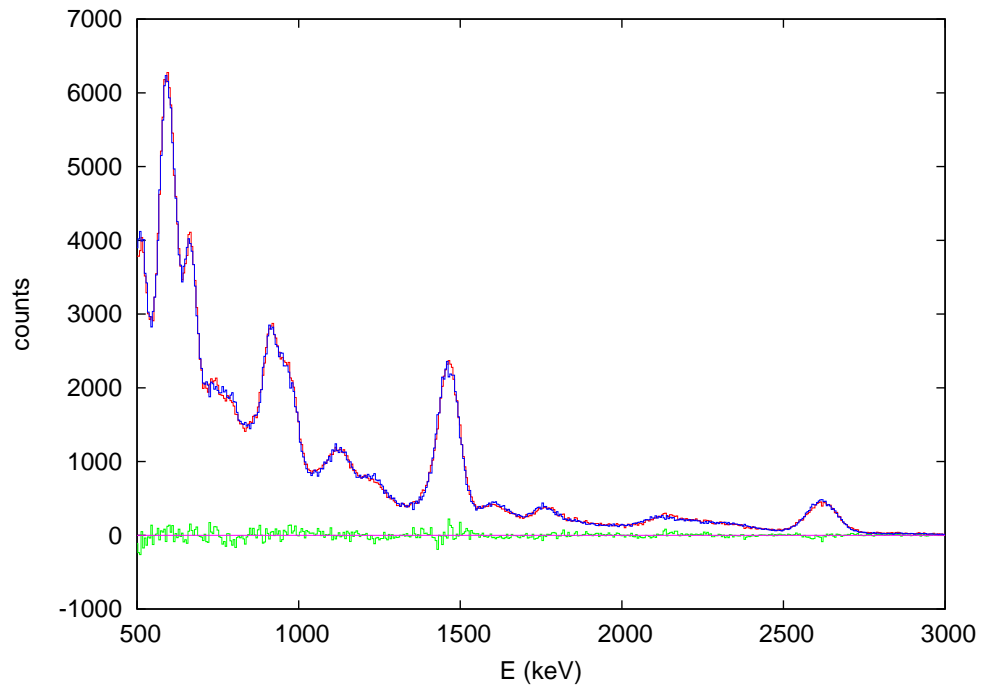


Figure 5: Result of the fit for a soil sample. The simulated spectrum (blue) reproduces quite well the experimental one (red). The green line represents the difference between the two spectra.

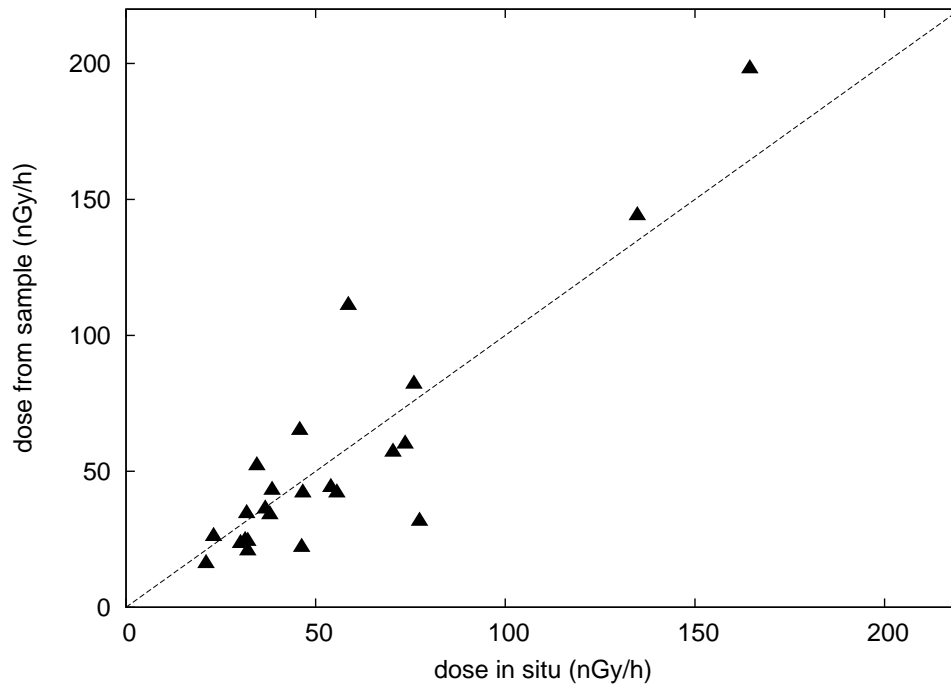


Figure 6: Comparison between the doses directly measured and those deduced by the content of radionuclides ($D_{nat}+D_{Cs}$). Equal doses lie on the dashed line.

Table 1: Results from the 56 measured soil samples. See text for explanations.

(*) lbs = light brown soil, dbs = dark brown soil, brs = brown soil, bs = black soil, rs = red soil, cb= calcareous breccia.

Sample	Soil (*)	Lat. 42° N +	Long. 13° E +	Alt. [m]	¹³⁷ Cs [Bq/kg]	K [%]	Th _{eq} [ppm]	U _{eq} [ppm]	D _{Cs} [nGy/h]	D _{nat} [nGy/h]	D _{cr} [nGy/h]	D _{tot} [nGy/h]	D _{situ} [nGy/h]
1	lbs	32' 46"	11' 51"	1.105	13.1	1.64	8.5	1.74	2.23	53	43	98	
2	lbs	32' 50"	15' 30"	980	58	1.68	8.8	1.93	9.9	55	41	105	
3	lbs	32' 53"	19' 09"	540	5.0	1.86	8.9	1.80	0.85	57	35.0	93	
4	lbs	32' 56"	22' 48"	1.320	18.2	1.22	5.9	1.40	3.09	38.6	47	88	47
5	lbs	30' 05"	11' 55"	940	11.4	1.77	8.7	2.15	1.94	57	40	99	
6	bs	30' 08"	15' 34"	1.120	99	0.69	8.0	1.46	16.8	37.3	43	97	
7	lbs	30' 11"	19' 14"	995	21.6	1.54	7.1	1.57	3.67	47	41	91	
8	lbs	30' 14"	22' 52"	1.120	5.4	1.24	6.3	1.62	0.92	41	43	85	56
9	lbs	30' 17"	26' 31"	1.370	51	1.80	9.1	1.92	8.6	57	48	113	
10	bs	27' 19"	08' 21"	1.180	75	1.08	18.2	1.73	12.8	69	44	126	
11	cb	27' 22"	11' 60"	1.180	6.0	0.064	0.68	0.49	1.02	5.3	44	50	
12	bs	27' 26"	15' 39"	805	135	0.73	8.0	5.0	23.0	58	38.2	119	
13	dbs	27' 29"	19' 17"	1.400	20.6	1.47	19.5	2.90	3.50	84	48	136	
14	cb	27' 32"	22' 56"	1.580	23.0	0.227	1.28	1.05	3.9	12.1	52	68	21
15	dbs	27' 35"	26' 35"	1.840	58	0.79	7.4	1.42	9.9	36.8	58	105	
16	cb	27' 38"	30' 14"	2.320	7.5	0.047	0.360	0.50	1.28	4.4	72	78	
17	bs	24' 40"	12' 05"	1.140	66	0.200	2.89	0.63	11.2	13.4	43	68	31
18	lbs	24' 44"	15' 43"	1.020	42	0.77	4.5	0.86	7.2	26.2	41	75	
19	dbs	24' 47"	19' 22"	938	10.7	1.74	58	5.0	1.82	196	40	238	165
20	bs	24' 50"	23' 00"	1.090	103	0.54	7.3	2.25	17.5	38.0	43	98	
21	bs	24' 53"	26' 39"	1.490	47	0.75	8.7	1.51	8.0	40	50	98	
22	brs	24' 56"	30' 18"	860	33.5	0.205	2.95	0.94	5.7	15.4	38.9	60	32
23	bs	24' 59"	33' 57"	1.560	37.0	0.76	9.0	2.01	6.3	44	52	102	

Table 1: (continued)

Sample	Soil (*)	Lat. 42° N +	Long. 13° E +	Alt. [m]	¹³⁷ Cs [Bq/kg]	K [%]	Th _{eq} [ppm]	U _{eq} [ppm]	D _{Cs} [nGy/h]	D _{nat} [nGy/h]	D _{cr} [nGy/h]	D _{tot} [nGy/h]	D _{situ} [nGy/h]
24	db	25' 01"	37' 36"	1.680	100	1.34	17.7	5.7	17.0	94	55	165	59
25	bs	25' 04"	41' 14"	1.680	64	0.82	9.1	3.07	10.9	51	55	116	
26	db	25' 07"	44' 53"	1.540	64	0.66	3.9	2.56	10.8	32.8	51	95	54
27	db	21' 58"	12' 09"	1.140	13.4	1.36	42	3.65	2.28	142	43	188	135
28	lbs+ cb	22' 02"	15' 48"	721	12.3	0.65	3.8	2.48	2.09	32.0	37.1	71	38
29	lbs	22' 05"	19' 26"	670	3.8	0.61	6.1	1.36	0.65	30.9	36.5	68	77
30	rs+cb	22' 08"	23' 04"	713	11.4	0.90	14.5	1.62	1.93	57	37.0	96	
31	br	22' 11"	26' 44"	680	49	0.45	5.1	1.31	8.2	26.1	36.6	71	32
32	bs	22' 14"	30' 22"	990	66	0.58	6.7	2.33	11.2	37.5	41	90	
33	db	22' 17"	34' 00"	1.310	13.4	0.280	2.64	1.76	2.28	20.2	47	69	
34	br	22' 20"	37' 39"	1.270	29.5	0.130	1.58	0.41	5.0	8.0	46	59	
35	bs	22' 22"	41' 18"	1.470	52	0.44	6.0	1.79	8.8	30.9	50	89	
36	rs	22' 25"	44' 56"	1.620	53	0.85	12.6	2.42	9.0	56	53	118	46
37	lbs	19' 20"	15' 52"	840	4.0	0.94	4.8	2.68	0.67	39	38.7	79	
38	lbs	19' 23"	19' 31"	810	73	1.79	13.7	2.08	12.4	69	38.2	120	76
39	lbs	19' 26"	23' 09"	830	28.1	0.340	3.4	1.13	4.8	19.3	38.5	63	32
40	lbs	19' 29"	26' 47"	587	10.1	1.67	8.8	2.09	1.72	56	35.5	93	70
41	lbs	19' 32"	30' 26"	615	21.3	0.48	5.5	2.21	3.62	32.5	35.8	72	37
42	bs	19' 35"	34' 04"	970	149	0.47	4.9	1.37	25.3	26.1	41	92	34
43	bs	19' 38"	37' 43"	1.200	26.2	1.00	16.3	2.06	4.5	65	44	114	
44	cb	19' 40"	41' 21"	1.230	13.1	0.43	5.2	0.90	2.23	23.7	45	71	23
45	rs	19' 42"	44' 59"	630	38	1.21	15.5	2.58	6.5	69	36.0	112	
46	bs	19' 45"	48' 38"	1.510	53	0.92	7.2	2.94	9.0	47	51	106	
47	bs	16' 38"	15' 57"	1.640	113	0.46	6.9	1.87	19.2	33.8	54	107	
48	br	16' 41"	19' 35"	1.305	67	0.70	9.7	1.89	11.4	44	46	102	
49	rs	16' 44"	23' 13"	1.600	2.30	0.98	9.3	2.36	0.39	49	53	102	
50	rs	16' 47"	26' 51"	1.225	25.9	1.39	44	2.80	4.4	145	45	194	

Table 1: (continued)

Sample	Soil (*)	Lat. 42° N +	Long. 13° E +	Alt. [m]	¹³⁷ Cs [Bq/kg]	K [%]	Th _{eq} [ppm]	U _{eq} [ppm]	D _{Cs} [nGy/h]	D _{nat} [nGy/h]	D _{cr} [nGy/h]	D _{tot} [nGy/h]	D _{situ} [nGy/h]
51	rs+cb	16' 50"	30' 30"	650	19.0	0.316	4.3	0.71	3.23	18.8	36.2	58	46
52	lbs	16' 53"	34' 08"	670	7.8	1.15	13.1	1.97	1.33	59	36.5	97	74
53	lbs	16' 55"	37' 46"	800	11.8	0.39	4.3	0.98	2.01	21.4	38.1	62	30
54	dbs	16' 58"	41' 24"	1.005	24.9	0.97	14.3	1.69	4.2	58	41	103	
55	lbs+ cb	17' 00"	45' 03"	390	13.7	0.75	9.2	1.31	2.33	40	33.7	76	39
56	bs	17' 03"	48' 41"	800	107	0.43	7.5	5.4	18.2	55	38.1	111	
Average					40.11	0.88	10.1	1.97	6.82	47.8	44.2	98.8	